

Measurement of the Generalized Polarizabilities of the Proton in Virtual Compton Scattering at $Q^2 = 0.92$ and 1.76 GeV^2

G. Laveissière,¹ L. Todor,² N. Degrande,³ S. Jaminion,¹ C. Jutier,^{1,2} R. Di Salvo,¹ L. Van Hooebeke,³ L. C. Alexa,⁴ B. D. Anderson,⁵ K. A. Aniol,⁶ K. Arundell,⁷ G. Audit,⁸ L. Auerbach,⁹ F. T. Baker,¹⁰ M. Baylac,⁸ J. Berthot,¹ P. Y. Bertin,¹ W. Bertozzi,¹¹ L. Bimbot,¹² W. U. Boeglin,¹³ E. J. Brash,⁴ V. Breton,¹ H. Breuer,¹⁴ E. Burtin,⁸ J. R. Calarco,¹⁵ L. S. Cardman,¹⁶ C. Cavata,⁸ C.-C. Chang,¹⁴ J.-P. Chen,¹⁶ E. Chudakov,¹⁶ E. Cisbani,¹⁷ D. S. Dale,¹⁸ C. W. de Jager,¹⁶ R. De Leo,¹⁹ A. Deur,^{1,16} N. d'Hose,⁸ G. E. Dodge,² J. J. Domingo,¹⁶ L. Elouadrhiri,¹⁶ M. B. Epstein,⁶ L. A. Ewell,¹⁴ J. M. Finn,⁷ K. G. Fissum,¹¹ H. Fonvieille,¹ G. Fournier,⁸ B. Frois,⁸ S. Frullani,¹⁷ C. Furget,²⁰ H. Gao,^{11,21} J. Gao,¹¹ F. Garibaldi,¹⁷ A. Gasparian,^{22,18} S. Gilad,¹¹ R. Gilman,^{23,16} A. Glamazdin,²⁴ C. Glashauser,²³ J. Gomez,¹⁶ V. Gorbenko,²⁴ P. Grenier,¹ P. A. M. Guichon,⁸ J. O. Hansen,¹⁶ R. Holmes,²⁵ M. Holtrop,¹⁵ C. Howell,²¹ G. M. Huber,⁴ C. E. Hyde-Wright,² S. Incerti,⁹ M. Iodice,¹⁷ J. Jardillier,⁸ M. K. Jones,^{7,16} W. Kahl,²⁵ S. Kato,²⁶ A. T. Katramatou,⁵ J. J. Kelly,¹⁴ S. Kerhoas,⁸ A. Ketikyan,²⁷ M. Khayat,⁵ K. Kino,²⁸ S. Kox,²⁰ L. H. Kramer,¹³ K. S. Kumar,²⁹ G. Kumbartzki,²³ M. Kuss,¹⁶ A. Leone,³⁰ J. J. LeRose,¹⁶ M. Liang,¹⁶ R. A. Lindgren,³¹ N. Liyanage,^{11,31} G. J. Lolos,⁴ R. W. Lourie,³² R. Madey,⁵ K. Maeda,²⁸ S. Malov,²³ D. M. Manley,⁵ C. Marchand,⁸ D. Marchand,⁸ D. J. Margaziotis,⁶ P. Markowitz,¹³ J. Marroncle,⁸ J. Martino,⁸ K. McCormick,^{2,23} J. McIntyre,²³ S. Mehrabyan,²⁷ F. Merchez,²⁰ Z. E. Meziani,⁹ R. Michaels,¹⁶ G. W. Miller,²⁹ J. Y. Mougey,²⁰ S. K. Nanda,¹⁶ D. Neyret,⁸ E. A. J. M. Offermann,¹⁶ Z. Papandreou,⁴ B. Pasquini,³³ C. F. Perdrisat,⁷ R. Perrino,³⁰ G. G. Petratos,⁵ S. Platchkov,⁸ R. Pomatsalyuk,²⁴ D. L. Prout,⁵ V. A. Punjabi,³⁴ T. Pussieux,⁸ G. Quémenér,^{7,20} R. D. Ransome,²³ O. Ravel,¹ J. S. Real,²⁰ F. Renard,⁸ Y. Roblin,^{1,16} D. Rowntree,¹¹ G. Rutledge,⁷ P. M. Rutt,²³ A. Saha,¹⁶ T. Saito,²⁸ A. J. Sarty,³⁵ A. Serdarevic,^{4,16} T. Smith,¹⁵ G. Smirnov,¹ K. Soldi,³⁶ P. Sorokin,²⁴ P. A. Souder,²⁵ R. Suleiman,^{5,11} J. A. Templon,¹⁰ T. Terasawa,²⁸ R. Tieulent,²⁰ E. Tomasi-Gustafsson,⁸ H. Tsubota,²⁸ H. Ueno,²⁶ P. E. Ulmer,² G. M. Urciuoli,¹⁷ M. Vanderhaeghen,^{37,7,16} R. Van De Vyver,³ R. L. J. Van der Meer,^{4,16} P. Vernin,⁸ B. Vlahovic,³⁶ H. Voskanyan,²⁷ E. Voutier,²⁰ J. W. Watson,⁵ L. B. Weinstein,² K. Wijesooriya,⁷ R. Wilson,³⁸ B. B. Wojtsekhowski,¹⁶ D. G. Zainea,⁴ W.-M. Zhang,⁵ J. Zhao,¹¹ and Z.-L. Zhou¹¹

(Jefferson Lab Hall A Collaboration)

¹Université Blaise Pascal/IN2P3, F-63177 Aubière, France

²Old Dominion University, Norfolk, Virginia 23529, USA

³University of Gent, B-9000 Gent, Belgium

⁴University of Regina, Regina, Saskatchewan S4S 0A2, Canada

⁵Kent State University, Kent, Ohio 44242, USA

⁶California State University, Los Angeles, California 90032, USA

⁷College of William and Mary, Williamsburg, Virginia 23187, USA

⁸CEA Saclay, F-91191 Gif-sur-Yvette, France

⁹Temple University, Philadelphia, Pennsylvania 19122, USA

¹⁰University of Georgia, Athens, Georgia 30602, USA

¹¹Massachusetts Institute of Technology, Cambridge, Massachusetts 02139, USA

¹²Institut de Physique Nucléaire, F-91406 Orsay, France

¹³Florida International University, Miami, Florida 33199, USA

¹⁴University of Maryland, College Park, Maryland 20742, USA

¹⁵University of New Hampshire, Durham, New Hampshire 03824, USA

¹⁶Thomas Jefferson National Accelerator Facility, Newport News, Virginia 23606, USA

¹⁷INFN, Sezione Sanità and Istituto Superiore di Sanità, 00161 Rome, Italy

¹⁸University of Kentucky, Lexington, Kentucky 40506, USA

¹⁹INFN, Sezione di Bari and University of Bari, 70126 Bari, Italy

²⁰Laboratoire de Physique Subatomique et de Cosmologie, F-38026 Grenoble, France

²¹Duke University, Durham, North Carolina 27706, USA

²²Hampton University, Hampton, Virginia 23668, USA

²³Rutgers, The State University of New Jersey, Piscataway, New Jersey 08855, USA

²⁴Kharkov Institute of Physics and Technology, Kharkov 61108, Ukraine

²⁵Syracuse University, Syracuse, New York 13244, USA

²⁶Yamagata University, Yamagata 990, Japan

²⁷Yerevan Physics Institute, Yerevan 375036, Armenia

²⁸Tohoku University, Sendai 980, Japan²⁹Princeton University, Princeton, New Jersey 08544, USA³⁰INFN, Sezione di Lecce, 73100 Lecce, Italy³¹University of Virginia, Charlottesville, Virginia 22901, USA³²State University of New York at Stony Brook, Stony Brook, New York 11794, USA³³DFNT, University of Pavia and INFN, Sezione di Pavia, ECT* Villazzano (Trento), Italy³⁴Norfolk State University, Norfolk, Virginia 23504, USA³⁵Florida State University, Tallahassee, Florida 32306, USA³⁶North Carolina Central University, Durham, North Carolina 27707, USA³⁷Institut fuer Kernphysik, University of Mainz, D-55099 Mainz, Germany³⁸Harvard University, Cambridge, Massachusetts 02138, USA

(Received 23 December 2003; published 14 September 2004)

We report a virtual Compton scattering study of the proton at low c.m. energies. We have determined the structure functions $P_{LL} - P_{TT}/\epsilon$ and P_{LT} , and the electric and magnetic generalized polarizabilities (GPs) $\alpha_E(Q^2)$ and $\beta_M(Q^2)$ at momentum transfer $Q^2 = 0.92$ and 1.76 GeV^2 . The electric GP shows a strong falloff with Q^2 , and its global behavior does not follow a simple dipole form. The magnetic GP shows a rise and then a falloff; this can be interpreted as the dominance of a long-distance diamagnetic pion cloud at low Q^2 , compensated at higher Q^2 by a paramagnetic contribution from πN intermediate states.

DOI: 10.1103/PhysRevLett.93.122001

PACS numbers: 13.60.Fz

The electric and magnetic polarizabilities of the nucleon describe its response to a static electromagnetic field. Contrary to atomic polarizabilities, which are of the size of the atomic volume [1], the proton electric polarizability α_E [2] is much smaller than 1 cubic fm, the volume scale of a nucleon. Such a small polarizability is a natural indication of the intrinsic relativistic character of the nucleon, as illustrated in a harmonic oscillator model [3]. The smallness of the proton magnetic polarizability β_M relative to α_E reflects a strong cancellation of paramagnetism and diamagnetism in the proton.

In virtual Compton scattering (VCS) $\gamma^* p \rightarrow \gamma p$ the polarizabilities become dependent on the momentum or the four-momentum transfer Q^2 of the virtual photon, as first introduced by Guichon *et al.* [4]. These generalized polarizabilities (GPs) can be seen as Fourier transforms of local polarization densities (electric, magnetic, and spin) [5]. Therefore they are a new probe of the nucleon dynamics, allowing us, e.g., to study the role of the pion cloud and quark core contributions to the nucleon GPs at various length scales. VCS can be accessed experimentally via exclusive photon electroproduction $ep \rightarrow ep\gamma$. After the NE-18 experiment [6] and the pioneering VCS experiment at MAMI [7], we performed the E93-050 $H(e, e'p)\gamma$ experiment [8] at the Thomas Jefferson National Accelerator Facility (JLab). We report low-energy expansion (LEX) analyses of our data up to pion threshold, and dispersion relation (DR) analyses of our data extending into the Δ -resonance region.

To lowest order in the fine structure constant α_{em} , the unpolarized $ep \rightarrow ep\gamma$ cross section at small q' is

$$d^5\sigma^{\text{EXP}} = d^5\sigma^{\text{BH+Bom}} + q'\phi\Psi_0 + \mathcal{O}(q'^2),$$

$$\Psi_0 = v_1\left(P_{LL} - \frac{1}{\epsilon}P_{TT}\right) + v_2P_{LT}, \quad (1)$$

where ϕ , v_1 , v_2 are kinematical coefficients defined in [9], q' is the final photon energy in the γp c.m. frame, and ϵ is the virtual photon polarization. $d^5\sigma^{\text{BH+Bom}}$ corresponds to the coherent sum of the Bethe-Heitler (BH) and the VCS Born amplitudes, and depends only on the elastic form factors G_E^p, G_M^p of the proton. This is a particular case of Low's low-energy theorem [10] for threshold photon production. The structure functions

$$P_{LL} - \frac{1}{\epsilon}P_{TT} = \frac{4M_p}{\alpha_{em}}G_E^p(Q^2)\alpha_E(Q^2) + [\text{spin-flip GPs}],$$

$$P_{LT} = -\frac{2M_p}{\alpha_{em}}\sqrt{\frac{q^2}{Q^2}}G_E^p(Q^2)\beta_M(Q^2) + [\text{spin-flip GPs}] \quad (2)$$

contain five of the six independent GPs [11,12]. These structure functions are defined at fixed q , the c.m. three-momentum of the VCS virtual photon. Equivalently, Q^2 in Eqs. (2) is defined in the $q' \rightarrow 0$ limit: $Q^2 = 2M_p(\sqrt{M_p^2 + q^2} - M_p)$.

The apparatus, running conditions, and analyses of the JLab experiment are detailed elsewhere [13–18]. An electron beam of 4.030 GeV energy was directed onto a 15 cm liquid hydrogen target. The two Hall A spectrometers were used to detect the scattered electron and the outgoing proton in coincidence, allowing the identification of the exclusive reaction $ep \rightarrow ep\gamma$ by the missing-mass technique. This experiment makes use of the full capabilities of the accelerator and the Hall A instrumentation [19]: 100% duty cycle, high resolution spectrometers, and high luminosities. We summarize our kinematics in Table I. Variables such as q' , or the c.m. polar and azimuthal angles θ and φ of the outgoing photon with respect to \vec{q} , are obtained by reconstructing

TABLE I. Kinematics of $ep \rightarrow ep\gamma$. We used data sets I-a and II for the LEX analyses and all data sets for the DR analyses.

Data set	Q^2 -Range (GeV ²)	W -Range
I-a	[0.85, 1.15]	Mostly $< \pi N$ threshold
I-b	[0.85, 1.15]	Mostly $\Delta(1232)$ resonance
II	[1.60, 2.10]	Mostly $< \pi N$ threshold

the missing particle. The acceptance calculation is provided by a dedicated Monte Carlo simulation [20] including a model cross section, resolution effects, and radiative corrections [21]. A number of cuts are applied in event analysis, especially to obtain a well-defined acceptance and to eliminate protons punching through the spectrometer entrance collimator.

We performed LEX analyses of the data sets I-a and II. The photon electroproduction cross section is determined as a function of q' , θ , and φ at a fixed value of q (1.080 and 1.625 GeV/ c) and ϵ (0.95 and 0.88, respectively). The effect of the GPs on the cross section is small, reaching at maximum 10%–15% below pion threshold. The method to extract the structure functions is deduced from Eq. (1), in which the (BH + Born) cross section is calculated using a recent parametrization of the proton form factors [22]. For each bin in (θ, φ) , we measure $d^5\sigma^{\text{EXP}}$ in several bins in q' , and extrapolate the quantity $\Delta\mathcal{M} = (d^5\sigma^{\text{EXP}} - d^5\sigma^{\text{BH+Born}})/(\phi q')$ to $q' = 0$, yielding the value of Ψ_0 . In our data, $\Delta\mathcal{M}$ does not exhibit any significant q' dependence, so the extrapolation to $q' = 0$ is done in each bin in (θ, φ) by averaging $\Delta\mathcal{M}$ over q' . The resulting Ψ_0 term is then fitted as a linear combination of two free parameters, which are the structure functions $P_{LL} - P_{TT}/\epsilon$ and P_{LT} (Fig. 1).

The systematic errors are calculated from four sources added quadratically: (1) ± 2 MeV uncertainty in beam energy, (2) ± 0.5 mrad uncertainty in horizontal angles, (3) $\pm 2.3\%$ uncertainty in overall absolute cross-section

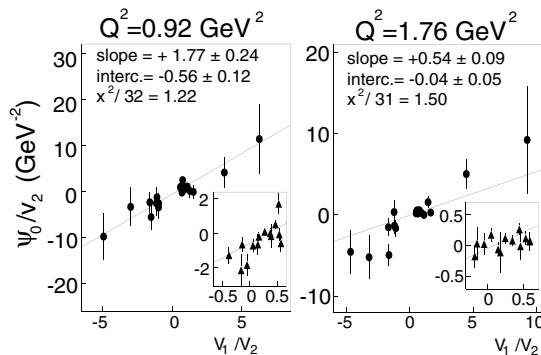


FIG. 1. A graphical representation of the LEX fit (straight line) for data sets I-a and II. Circles correspond to out-of-plane data, and the inner plot is a zoom on the lepton plane data (triangles). Ψ_0 , ν_1 , and ν_2 are defined in the text.

normalization, and (4) $\pm 2\%$ uncertainty due to possible cross-section shape distortions. The value of the reduced χ^2 of the fit (Fig. 1) is one measure of the validity of the LEX in our kinematics. The LEX results for the structure functions are summarized in Table II.

We performed DR analyses of the data sets I-a and II, and also I-b including data from πN threshold through the Δ resonance. In the DR formalism of Pasquini *et al.* [23], the VCS amplitude is determined by unitarity from the MAID $\gamma^{(*)}p \rightarrow N\pi$ multipoles [24], plus asymptotic terms $\Delta\alpha$, $\Delta\beta$ which are unconstrained phenomenological contributions to the GPs $\alpha_E(Q^2)$ and $\beta_M(Q^2)$. $\Delta\alpha$, $\Delta\beta$ are parametrized as follows:

$$\Delta\alpha(Q^2) = \alpha_E(Q^2) - \alpha_E^{\pi N}(Q^2) = \frac{[\alpha_E^{\text{exp}} - \alpha_E^{\pi N}]_{Q^2=0}}{(1 + Q^2/\Lambda_\alpha^2)^2} \quad (3)$$

(same relation for $\Delta\beta$ with parameter Λ_β) where $\alpha_E^{\pi N}$ ($\beta_M^{\pi N}$) is the πN dispersive contribution evaluated from MAID, α_E^{exp} (β_M^{exp}) is the experimental value at $Q^2 = 0$ [2], and the mass coefficients Λ_α and Λ_β are free parameters. Theoretically, the choice of the dipole form in Eq. (3) is not compulsory. More fundamentally, the DR model provides a rigorous treatment of the higher order terms in the VCS amplitude up to the $N\pi\pi$ threshold, by including resonances in the πN channel. In the region of the $\Delta(1232)$ resonance, these higher order terms become dominant over the lowest order GPs given by the LEX.

The DR analysis consists in fitting the free parameters Λ_α and Λ_β to our cross-section data. This yields the value of the GPs $\alpha_E(Q^2)$ and $\beta_M(Q^2)$ using Eq. (3). This also yields the value of the structure functions of Eqs. (2) since the DR model predicts all the spin-flip GPs [23]. Our DR results are presented in Tables II and III. The systematic uncertainties are calculated from the same sources as in the LEX analyses. The error bars differ from one data set

TABLE II. Compilation of the VCS structure functions. In all cases the first error is statistical, and the second one is the total systematic error.

	Q^2 (GeV ²)	ϵ	$P_{LL} - P_{TT}/\epsilon$ (GeV ⁻²)	P_{LT} (GeV ⁻²)
Ref.	Previous experiments			
[2]	0		$81.3 \pm 2.0 \pm 3.4$	$-5.4 \pm 1.3 \pm 1.9$
[7]	0.33	0.62	$23.7 \pm 2.2 \pm 4.3$	$-5.0 \pm 0.8 \pm 1.8$
Set	This experiment, LEX Analyses			
I-a	0.92	0.95	$1.77 \pm 0.24 \pm 0.70$	$-0.56 \pm 0.12 \pm 0.17$
II	1.76	0.88	$0.54 \pm 0.09 \pm 0.20$	$-0.04 \pm 0.05 \pm 0.06$
Set	This experiment, DR Analyses			
I-a	0.92	0.95	$1.70 \pm 0.21 \pm 0.89$	$-0.36 \pm 0.10 \pm 0.27$
I-b	0.92	0.95	$1.50 \pm 0.18 \pm 0.19$	$-0.71 \pm 0.07 \pm 0.05$
II	1.76	0.88	$0.40 \pm 0.05 \pm 0.16$	$-0.09 \pm 0.02 \pm 0.03$

TABLE III. The dipole mass parameters Λ_α and Λ_β obtained by fitting the three data sets independently, and the electric and magnetic GPs evaluated at $Q^2 = 0.92 \text{ GeV}^2$ (data sets I-a, I-b) and 1.76 GeV^2 (data set II). The first and second errors are statistical and total systematic errors, respectively.

Data set	Λ_α (GeV)	Λ_β (GeV)
I-a	$0.741 \pm 0.040 \pm 0.175$	$0.788 \pm 0.041 \pm 0.114$
I-b	$0.702 \pm 0.035 \pm 0.037$	$0.632 \pm 0.036 \pm 0.023$
II	$0.774 \pm 0.050 \pm 0.149$	$0.698 \pm 0.042 \pm 0.077$
Data set	$\alpha_E(Q^2)$ (10^{-4} fm^3)	$\beta_M(Q^2)$ (10^{-4} fm^3)
I-a	$1.02 \pm 0.18 \pm 0.77$	$0.13 \pm 0.15 \pm 0.42$
I-b	$0.85 \pm 0.15 \pm 0.16$	$0.66 \pm 0.11 \pm 0.07$
II	$0.52 \pm 0.12 \pm 0.35$	$0.10 \pm 0.07 \pm 0.12$

to another, due to differences in phase space coverage and in sensitivity to both the physics and the sources of systematic errors. The reasonably good χ^2 of the DR fits (1.3 to 1.5) indicates that the DR model allows a reliable extraction of GPs in our kinematics, both below and above pion threshold.

Figure 2 shows our DR extraction of the GPs $\alpha_E(Q^2)$ and $\beta_M(Q^2)$, together with the point at $Q^2 = 0$ [2] and the points derived from LEX analyses. The latter are obtained by subtracting the spin-flip polarizability predictions [23] to the structure functions of Eqs. (2). This involves some model dependence, which is not presently taken into account in the error bars.

The solid curves in Fig. 2 are the full DR calculations, split into their dispersive πN contributions (dashed line) and the remaining asymptotic contributions of Eq. (3) (dash-dotted line) for $\Lambda_\alpha = 0.70 \text{ GeV}$ and $\Lambda_\beta = 0.63 \text{ GeV}$, as fitted to the JLab data set I-b. The πN contribution to the magnetic polarizability in Fig. 2(b) is strongly paramagnetic, predominantly arising from the $\Delta(1232)$ resonance. In the DR formalism, this is canceled by a strong diamagnetic term $\Delta\beta$ originating from the σ -meson t -channel exchange. The interpretation of $\Delta\beta$ as the contribution of a long-distance pion cloud is further supported by the fact that the fitted scale parameter $\Lambda_\beta = 0.63 \text{ GeV}$ is smaller than the elastic form factor dipole parameter $\Lambda = 0.84 \text{ GeV}$. The dotted curves in Fig. 2 result from the full DR calculation, evaluated with $\Lambda_\alpha = 1.79 \text{ GeV}$ and $\Lambda_\beta = 0.51 \text{ GeV}$, which reproduces the MAMI LEX data. The data for $\alpha_E(Q^2)$ disagree strongly with the simple dipole ansatz for the contribution $\Delta\alpha$. It should be noted that our DR analysis is basically insensitive to the particular choice of form of $\Delta\alpha$ and $\Delta\beta$, since our fits are performed independently in two small ranges of Q^2 . Finally, we point out that the ηN and $\pi\pi N$ channels, which must contribute to $\Delta\alpha$, have resonances [$S_{11}(1535)$ and $D_{13}(1520)$, respectively] with transition form factors that do not follow a simple dipole Q^2 dependence [25,26].

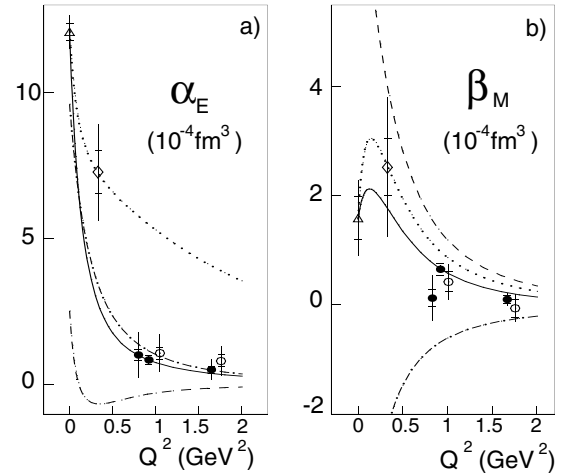


FIG. 2. Compilation of the data on electric (a) and magnetic (b) GPs. Data points are from Ref. [2] (Δ), the LEX analysis of MAMI [7] (\diamond), and the present LEX (\circ) and DR (\bullet) analyses of JLab. Some JLab points are shifted in abscissa for better visibility. The inner error bar is statistical; the outer one is the total error (statistical plus systematic). The curves show calculations in the DR model (see text).

In summary, we studied the process $ep \rightarrow ep\gamma$ at JLab. With data below pion threshold we applied the LEX, and for data extending through the Δ resonance we applied the DR formalism to extract the generalized polarizabilities. The different analyses are consistent, and the results give new insight into the correlations between spatial and dynamical variables in the proton. Other experiments at low energy will measure the VCS structure functions at low Q^2 [27,28] and separate the six GPs via double polarization measurements [28,29].

We thank the JLab accelerator staff and the Hall A technical staff for their dedication. This work was supported by DOE Contract No. DE-AC05-84ER40150 under which the Southeastern Universities Research Association (SURA) operates the Thomas Jefferson National Accelerator Facility. We acknowledge additional grants from the U.S. DOE and NSF, the French CNRS and CEA, the Conseil Régional d'Auvergne, the FWO-Flanders (Belgium), and the BOF-Gent University. We thank the INT (Seattle) and ECT* (Trento) for the organization of VCS workshops.

- [1] V. A. Dzuba, V.V. Flambaum, and O. P. Sushkov, Phys. Rev. A **56**, R4357 (1997).
- [2] V. Olmos de Leon *et al.*, Eur. Phys. J. A **10**, 207 (2001).
- [3] B. R. Holstein, D. Drechsel, B. Pasquini, and M. Vanderhaeghen, Phys. Rev. C **61**, 034316 (2000).
- [4] P. A. M. Guichon, G. Q. Liu, and A. W. Thomas, Nucl. Phys. **A591**, 606 (1995).
- [5] A. I. Lvov, S. Scherer, B. Pasquini, C. Unkmeir, and D. Drechsel, Phys. Rev. C **64**, 015203 (2001).

- [6] J. F. J. van den Brand *et al.*, Phys. Rev. D **52**, 4868 (1995).
[7] J. Roche *et al.*, Phys. Rev. Lett. **85**, 708 (2000).
[8] P. Y. Bertin *et al.*, Report No. E93-050, 1993, <http://hallaweb.jlab.org/experiment/E93-050/vcs.html>.
[9] P. A. M. Guichon and M. Vanderhaeghen, Prog. Part. Nucl. Phys. **41**, 125 (1998).
[10] F. E. Low, Phys. Rev. **110**, 974 (1958).
[11] D. Drechsel, G. Knochlein, A. Metz, and S. Scherer, Phys. Rev. C **55**, 424 (1997).
[12] D. Drechsel, G. Knochlein, A. Y. Korchin, A. Metz, and S. Scherer, Phys. Rev. C **57**, 941 (1998).
[13] G. Laveissière *et al.*, Phys. Rev. C **69**, 045203 (2004).
[14] N. Degrande, Ph.D. thesis, Gent University, 2001.
[15] S. Jaminion, Ph.D. thesis, Université Blaise Pascal of Clermont-Fd, 2001, DU 1259.
[16] C. Jutier, Ph.D. thesis, Old Dominion University and Université Blaise Pascal of Clermont-Fd, 2001, DU 1298.
[17] G. Laveissière, Ph.D. thesis, Université Blaise Pascal of Clermont-Fd, 2001, DU 1309.
[18] L. Todor, Ph.D. thesis, Old Dominion University, 2000.
[19] J. Alcorn *et al.*, Nucl. Instrum. Methods Phys. Res., Sect. A **522**, 294 (2004).
[20] L. Van Hoorebeke *et al.* (to be published).
[21] M. Vanderhaeghen, J. M. Friedrich, D. Lhuillier, D. Marchand, L. Van Hoorebeke, and J. Van de Wiele, Phys. Rev. C **62**, 025501 (2000).
[22] E. J. Brash, A. Kozlov, S. Li, and G. M. Huber, Phys. Rev. C **65**, 051001 (2002).
[23] B. Pasquini, M. Gorchtein, D. Drechsel, A. Metz, and M. Vanderhaeghen, Eur. Phys. J. A **11**, 185 (2001).
[24] D. Drechsel, O. Hanstein, S. S. Kamalov, and L. Tiator, Nucl. Phys. **A645**, 145 (1999).
[25] CLAS Collaboration, R. Thompson *et al.*, Phys. Rev. Lett. **86**, 1702 (2001).
[26] L. Tiator *et al.*, nucl-th/0310041.
[27] J. Shaw *et al.*, MIT-Bates Proposal No. E97-03, 1997.
[28] H. Merkel and N. d'Hose, spokespersons, MAMI Proposal, 2000.
[29] M. Vanderhaeghen, Phys. Lett. B **402**, 243 (1997).